Quaternary Science Reviews 63 (2013) 73–82

Contents lists available at SciVerse ScienceDirect

Quaternary Science Reviews

journal homepage: www.elsevier.com/locate/quascirev

Revised estimates of Greenland ice sheet thinning histories based on ice-core records

Benoit S. Lecavalier [a,*], Glenn A. Milne [a,b], Bo M. Vinther [c], David A. Fisher [b,d], Arthur S. Dyke [d], Matthew J.R. Simpson [e]

[a] Department of Physics, University of Ottawa, Ottawa, Ontario, Canada K1N 6N5
[b] Department of Earth Sciences, University of Ottawa, Canada
[c] Centre for Ice and Climate, Niels Bohr Institute, University of Copenhagen, Denmark
[d] Geological Survey of Canada, NRCan, Ottawa, Canada
[e] Norwegian Mapping Authority, Hønefoss, Norway

ARTICLE INFO

Article history:
Received 22 June 2012
Received in revised form
29 November 2012
Accepted 30 November 2012
Available online 21 January 2013

Keywords:
Greenland ice sheet
Ice core isotope records
Relative sea level
Glacial isostatic adjustment
Ice sheet reconstruction

ABSTRACT

Ice core records were recently used to infer elevation changes of the Greenland ice sheet throughout the Holocene. The inferred elevation changes show a significantly greater elevation reduction than those output from numerical models, bringing into question the accuracy of the model-based reconstructions and, to some extent, the estimated elevation histories. A key component of the ice core analysis involved removing the influence of vertical surface motion on the $\delta^{18}O$ signal measured from the Agassiz and Renland ice caps. We re-visit the original analysis with the intent to determine if the use of more accurate land uplift curves can account for some of the above noted discrepancy. To improve on the original analysis, we apply a geophysical model of glacial isostatic adjustment calibrated to sea-level records from the Queen Elizabeth Islands and Greenland to calculate the influence of land height changes on the $\delta^{18}O$ signal from the two ice cores. This procedure is complicated by the fact that $\delta^{18}O$ contained in Agassiz ice is influenced by land height changes distant from the ice cap and so selecting a single location at which to compute the land height signal is not possible. Uncertainty in this selection is further complicated by the possible influence of Innuitian ice during the early Holocene (12–8 ka BP). Our results indicate that a more accurate treatment of the uplift correction leads to elevation histories that are, in general, shifted down relative to the original curves at GRIP, NGRIP, DYE-3 and Camp Century. In addition, compared to the original analysis, the 1-σ uncertainty is considerably larger at GRIP and NGRIP. These changes reduce the data-model discrepancy reported by Vinther et al. (2009) at GRIP, NGRIP, DYE-3 and Camp Century. A more accurate treatment of isostasy and surface loading also acts to improve the data-model fits such that the residuals at all four sites for the period 8 ka BP to present are significantly reduced compared to the original analysis. Prior to 8 ka BP, the possible influence of Innuitian ice on the inferred elevation histories prevents a meaningful comparison.

1. Introduction

1.1. Holocene thinning of the Greenland ice sheet

Vinther et al. (2009) applied a novel procedure to determine ice surface elevation curves of the Greenland ice sheet (GrIS) at four ice core locations (GRIP, NGRIP, DYE-3 and Camp Century; see Fig. 1a). These observationally-constrained curves depict a Holocene thinning history that is considerably more rapid and of greater amplitude than that indicated from the output of numerical ice models. The discrepancy is large, several hundred metres at some core sites, and brings into question the accuracy of both the ice models and the thinning curves. This paper revisits two aspects of the Vinther et al. (2009) (shortened to Vinther et al. in the following) analysis in order to assess their impact on the resulting thinning curves and whether it can account for some of the discrepancy mentioned above.

In the original Vinther et al. analysis, the thinning curves were derived by considering the climate records in two ice caps, Agassiz and Renland (henceforth AR), situated on either side of Greenland (Fig. 1a). After estimating and removing the contribution of vertical land motion to the AR $\delta^{18}O$ records, the elevation-corrected $\delta^{18}O$

* Corresponding author.
E-mail address: bleca056@uottawa.ca (B.S. Lecavalier).

0277-3791/$ – see front matter © 2013 Elsevier Ltd. All rights reserved.
http://dx.doi.org/10.1016/j.quascirev.2012.11.030

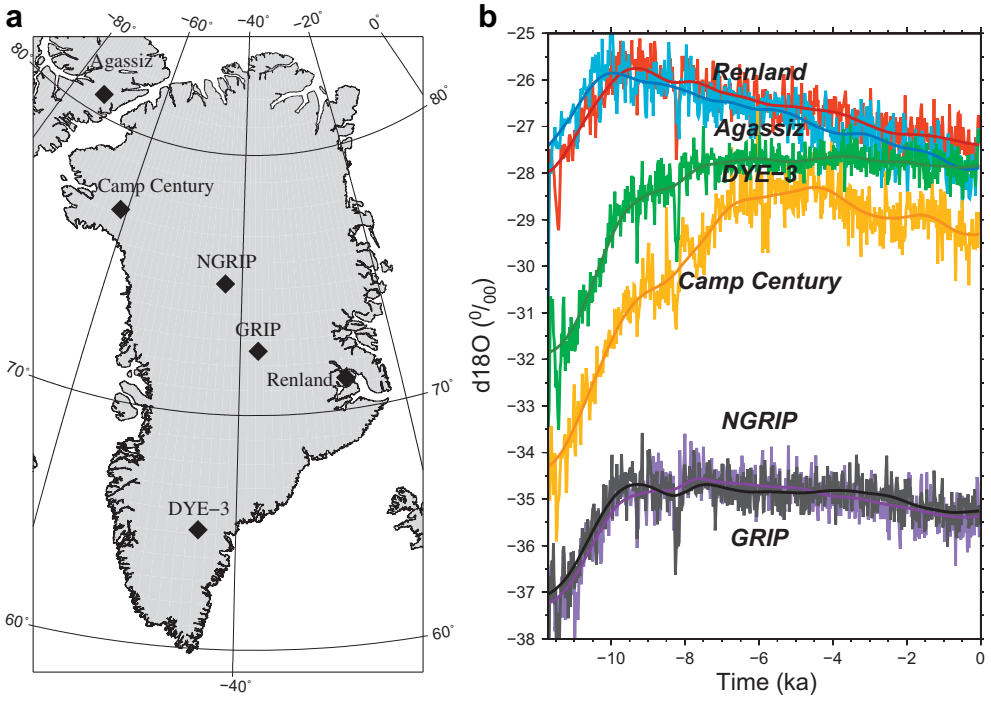

Fig. 1. (a) The location and names of the relevant ice cores discussed in this study. (b) The synchronized $\delta^{18}O$ records for all the sites shown in (a); both raw and smoothed (Gaussian filtered) signals are shown.

records were applied to infer a homogeneous $\delta^{18}O$ field for the entire region. As discussed below, the AR ice caps have topographical constraints that limit their former vertical extent (thickness) (Johnsen et al., 1992; Fisher et al., 1995). Consequently, no elevation correction for thickness changes of either ice cap was applied in the Vinther et al. analysis.

A synchronized stratigraphical timescale for the Holocene (GICC05) of DYE-3, GRIP, NGRIP, Camp Century, Renland and Agassiz was made by matching prominent volcanic reference horizons in electrical conductivity measurements (Vinther et al., 2006, 2008) and gaussian filtered to capture millennium scale variations (Fig. 1b). By removing the uplift-corrected AR $\delta^{18}O$ records from the $\delta^{18}O$ records at Camp Century, DYE-3, GRIP and NGRIP, changes in ice surface elevation were isolated at these sites. The two aspects of the original analysis investigated in this paper are (i) the accuracy of the elevation corrections applied at the AR ice caps and (ii) the resulting inference and application of a $\delta^{18}O$ profile for the entire region.

The main contribution of this study is to assess the accuracy of the land uplift correction applied in the original Vinther et al. analysis and determine the impact of this on the estimated thinning curves. The post glacial uplift estimated for AR in Vinther et al. was conducted using observations of past changes in relative sea level (RSL) in nearby fiords. The Agassiz bedrock elevation history is based on a set of data dating back to 9.5 ka before present (BP; relative to AD, 2000) and extrapolated to 11.7 ka BP using the observed exponential decay time for RSL change (Dyke and Peltier, 2000). Similarly, the uplift estimated for Renland was obtained using past changes in sea level in nearby fiords (Funder, 1978). Using RSL as a proxy for vertical land motion will lead to some degree of error due to the contribution from vertical motion of the sea surface. We improve upon this method here by modelling RSL observations from Ellesmere and Devon Islands and north–west Greenland (Fig. 2) to calibrate a glacial isostatic adjustment (GIA) sea-level model for this region. The calibrated model is then applied to determine land uplift histories at the appropriate locations (not necessarily at the ice core sites – see Section 1.2).

The second contribution of this study relates to the temperature reconstruction from the individual AR $\delta^{18}O$ records and the

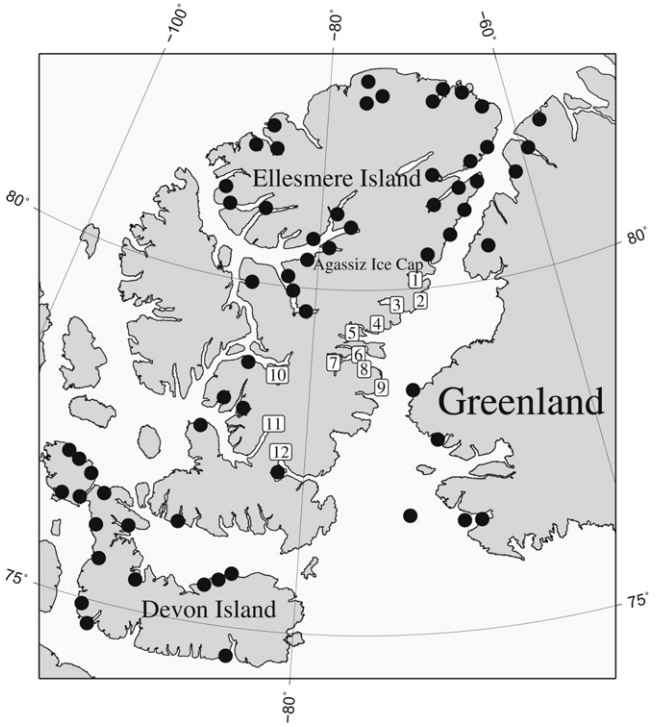

Fig. 2. The distribution of sites (black circles and 12 numbered sites) across the Canadian Arctic and Greenland which had sufficient sea level proxy information to constrain our glacial isostatic adjustment (GIA) model.

spatially varying $\delta^{18}O$ history generated across Greenland. The revised land uplift corrections result in a substantial difference between the $\delta^{18}O$ records inferred from the AR cores. Therefore, instead of averaging this to create a homogeneous $\delta^{18}O$ profile for the region (which would result in large error bars on the inferred thinning curves), we use the differences between the AR records to infer a spatial gradient in $\delta^{18}O$ and apply this non-homogeneous signal to estimate thinning curves at the Greenland ice core sites.

As stated above, the over-arching aim of this work is to assess whether these extensions of the original Vinther et al. analysis can account for at least some of the discrepancy between the inferred and modelled Holocene thinning of the GrIS.

1.2. Interpreting $\delta^{18}O$ from the Renland and Agassiz ice caps

A key aspect of the Vinther et al. study is the estimation of temperature from observations of $\delta^{18}O$ in AR ice. The $\delta^{18}O$ values obtained from ice cores are affected by air temperature, location of the moisture source, the pathways by which the moisture is transported, and precipitation (Dansgaard, 1961). Understanding which of these processes are primary versus secondary drivers of $\delta^{18}O$ changes is crucial for assessing the accuracy of the inferred elevation histories. It has been observed that numerous northern hemisphere $\delta^{18}O$ records from ice cores extending back through and beyond the Holocene are described to first order by two effects that relate to changes in air temperature: an altitude effect ($-0.6‰$ per 100 m) and a latitude effect ($-0.54‰$ per degree N) (Dansgaard, 1961; Johnsen and White, 1989). It is through the former that elevation of the ice surface, in this case dominated by GIA, influences the adiabatic cooling of the local air mass in which precipitation induced fractionation occurs and ultimately influences the $\delta^{18}O$ signal. It is also noteworthy that the AR $\delta^{18}O$ records are surprisingly similar considering the distance between the sites (Funder, 1978; Koerner, 1979).

The Renland ice cap is located on a high plateau with steep descents down to the Scoresbysund Fjord and the surrounding terrain, thereby limiting the lateral extent of the ice cap. From considering the equilibrium profile of an ice cap, this constraint on the lateral extent of the base limits the maximum thickness that the ice cap can achieve over millennium timescales. Although Renland can thin beyond this maximum equilibrium thickness, there is strong evidence that it has not done so during the Holocene. The present maximum extent of Renland associated with relatively warm air temperature and high precipitation is most likely indicative of its extent during the Holocene when, in general, temperatures were relatively high. Because this part of the GrIS receives some of the highest accumulation rates, it makes it difficult to argue for a significant thinning of the ice cap during the Holocene. Indeed, conceptual models of the recent glacial–interglacial transition, with increased warming and accumulation resulted in no more than 30 m of change to Renland's thickness (Vialov, 1958; Johnsen et al., 1992). Furthermore, the continuous stratigraphy of the Renland ice core, including basal Eemian ice, indicates very long survival (Johnsen et al., 1992). We therefore think it is reasonable to assume that the Renland $\delta^{18}O$ record is not significantly influenced by altitude variation through changes in ice thickness.

The Agassiz ice cap is found on the central part of Ellesmere Island (Fig. 2), where two ice cores (A84/A87) were drilled on a local dome. The dome is located at the point of highest bedrock elevation which has resulted in the formation of a Raymond bump in the layering of the ice cap (Vinther et al., 2008). Ice flow between Agassiz boreholes in connection with wind scouring effects has been modelled and the results illustrate the relative stability of the ice cap over the Holocene (Fisher et al., 1995). The melt records from the Agassiz ice cores display the response of the ice cap to the Holocene thermal maximum (HTM) and suggest thinning of the ice cap on the order of 100 m at that time (Fisher et al., 1995). However, we note that changes in thickness of the ice cap do not affect the $\delta^{18}O$ content of Agassiz ice; there is no evidence of local altitude effects (e.g. from Agassiz ice thickness changes) on the observed $\delta^{18}O$ (Koerner, 1979; Koerner and Fisher, 1990; Fisher, 1992). The air masses that precipitate onto the Agassiz ice cap primarily originate in Baffin Bay. These are first elevated along the eastern shores of Ellesmere Island and since there is no inland topography capable of forcing the air masses higher, the $\delta^{18}O$ from Agassiz ice is more sensitive to elevation changes along this shoreline (Fisher, 1990). This pattern of air mass elevation and isotopic fractionation has several important implications: (1) Agassiz thickness changes on the order of 100 m are of no consequence to a Vinther et al. type analysis, the elevation correction associated with land uplift should not be calculated at the drill sites, but rather at a location along the coastline of Ellesmere Island and (2) the position at which the correction should be estimated will change throughout the Holocene due to the influence of Innuitian ice on the topography of southern Ellesmere Island. Thinning of Innuitian ice will, in fact, dominate over isostatic land uplift during the early Holocene. This component of the Agassiz elevation correction, which was overlooked in the original analysis, will add considerably to the uncertainty in the estimated thinning curves for the early Holocene. As discussed in Section 2, these issues complicate the task of arriving at a well-constrained elevation correction for the Agassiz $\delta^{18}O$ record prior to 8 ka BP.

2. Methodology

2.1. Agassiz and Renland land uplift correction

As described above, we used a GIA model to remove the land uplift contribution to the AR $\delta^{18}O$ data. We calibrated the model using RSL data from Arctic Canada and Greenland. Our GIA model computes Earth deformation, gravity and sea-level changes resulting from the interaction between ice sheets and the solid Earth (e.g. Farrell and Clark, 1976; Milne and Mitrovica, 1998; Mitrovica and Milne, 2003). The model uses two primary inputs, an ice model and an Earth model. Two ice models were used: ICE-5G (Peltier, 2004) and a revised version of ICE-5G with the Greenland component removed (referred to as GrB; Tarasov and Peltier, 2002) and replaced by a more recent reconstruction of this ice sheet (referred to as Huy2; Simpson et al., 2009). A spherically symmetric viscoelastic rotating Earth model was adopted with the elastic and density structure given by the seismic Preliminary Reference Earth Model (Dziewonski and Anderson, 1981), and the viscous structure more crudely defined into three shells: lithosphere, upper mantle, and lower mantle. The lithosphere was assigned a relatively high viscosity to simulate an elastic outer shell with a thickness that was varied when seeking an optimal model fit to the RSL data. The upper-lower mantle boundary was defined at a depth of 670 km and the viscosity in these two regions used as free parameters when modelling the RSL data (e.g. Simpson et al., 2009).

RSL data from Ellesmere, Devon Islands and Greenland were used to determine optimal Earth model parameters (lithospheric thickness, upper and lower mantle viscosity) for each ice model. A total of 171 Earth viscosity models were considered in seeking an optimal data-model fit. The RSL data are generally of low precision as the reconstructions are based on, for the most part, shells, whale bones and drift wood (e.g. Dyke and Peltier, 2000). This type of evidence permits only upper and lower limits to be placed on RSL (see Fig. 3). The results of the Earth model calibration exercise are given in Section 3, along with the revised uplift corrections.

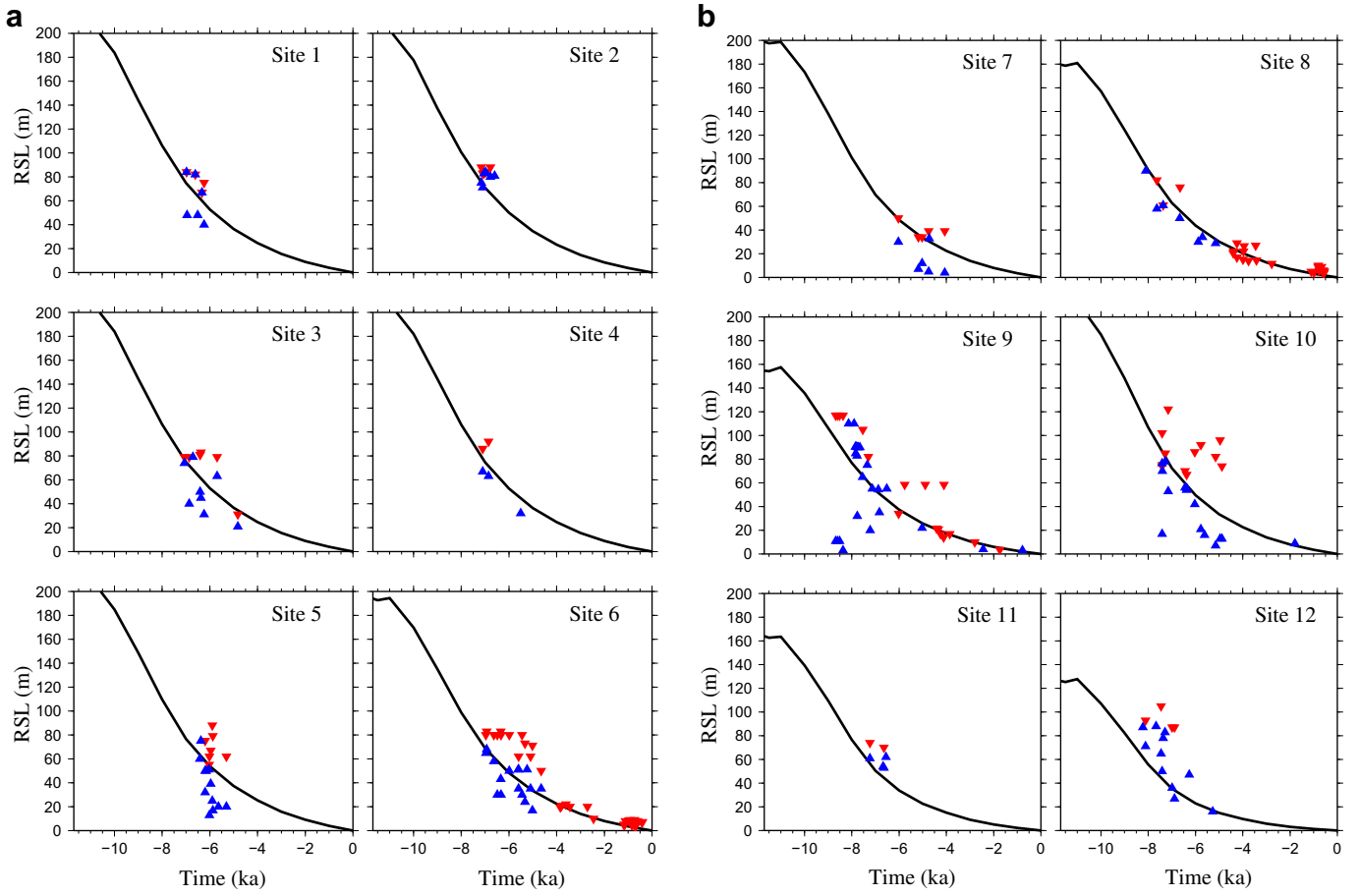

Fig. 3. Relative sea-level observations and predictions at the 12 sites which are of greatest relevance to the GIA/RSL model. The red (down pointing) and blue triangles (up pointing) represent an upper and lower bound on sea level, respectively. The sea-level curve on each graph was generated using ICE-5G as the ice model and an optimal Earth model with lithosphere thickness of 71 km, upper mantle viscosity of 3×10^{20} Pa s, and lower mantle viscosity of 10^{21} Pa s. (For interpretation of the references to colour in this figure legend, the reader is referred to the web version of this article.)

2.2. Holocene temperature and thinning reconstructions

The reconstruction of Holocene surface air temperatures from the AR $\delta^{18}O$ records requires corrections for both uplift and changes in $\delta^{18}O$ content of sea water (Waelbroeck et al., 2002). A forward modelling method is used to calibrate the AR corrected $\delta^{18}O$ records with the borehole temperature profiles from GRIP, NGRIP, DYE-3 and Camp Century by numerically solving the differential equation for heat conduction in moving ice yielding a $^{\circ}C/\delta^{18}O$ slope of 2.1 ± 0.2 (Johnsen, 1977; Dahl-Jensen and Johnsen, 1986; Johnsen et al., 1992; Gundestrup et al., 1993; Dahl-Jensen et al., 1998, 2003; Vinther et al., 2009).

In the Vinther et al. study, based on the original uplift corrections on the AR ice caps, the two $\delta^{18}O$ records were strikingly similar, therefore, the records were averaged to ultimately yield a single temperature reconstruction for the entire region. Using the $\delta^{18}O$ signal for the region, variations in ice elevation at each Greenland core site was isolated and subsequently corrected for upstream effects at NGRIP, DYE-3, and Camp Century, yielding the Holocene thinning curves (Reeh et al., 1985; Buchardt and Dahl-Jensen, 2007; Vinther et al., 2009). An important consequence in adopting a single $\delta^{18}O$ record is that the residual between the uplift-corrected AR $\delta^{18}O$ records translates into an uncertainty in the estimated thinning curves (of amplitude ± 25 m in the original analysis).

When applying more accurate uplift curves (see below) it was found that the AR $\delta^{18}O$ records diverged from one another by a greater amount than in the original study (Vinther et al., 2009, Fig. 5), especially after reducing the AR records to the same height to remove the elevation difference between AR. This $\delta^{18}O$ discrepancy translates into an uncertainty in the final thinning curves that would be much greater than that obtained in the original analysis. As a consequence, rather than average the AR records, we have extended the original study to account for a spatial gradient in the $\delta^{18}O$ between the ice cores and thus reduce the uncertainty resulting from the AR $\delta^{18}O$ discrepancy. The difference in the uplift-corrected height synchronized $\delta^{18}O$ records from the AR cores were applied to generate a linear $\delta^{18}O$ profile from Renland to Agassiz, along with a temperature reconstruction at the Renland and Agassiz cores. A site specific $\delta^{18}O$ record is deduced at GRIP, NGRIP, DYE-3 and Camp Century by interpolating/extrapolating the Renland to Agassiz $\delta^{18}O$ records. Based on these site specific $\delta^{18}O$ records, new thinning curves are derived.

3. Results and discussion

3.1. GIA correction

RSL predictions for a subset of sites are shown in Fig. 3a and b (numbered sites in Fig. 2); the model fits are shown at these particular sites since it is along this section of Ellesmere (east coast, south of the Agassiz ice cap) that the vertical land motion correction is to be applied. Red and blue data points indicate upper and lower bounds (limiting dates) for sea-level, respectively. The elevation of the variety of sea-level indicators collected in the Arctic

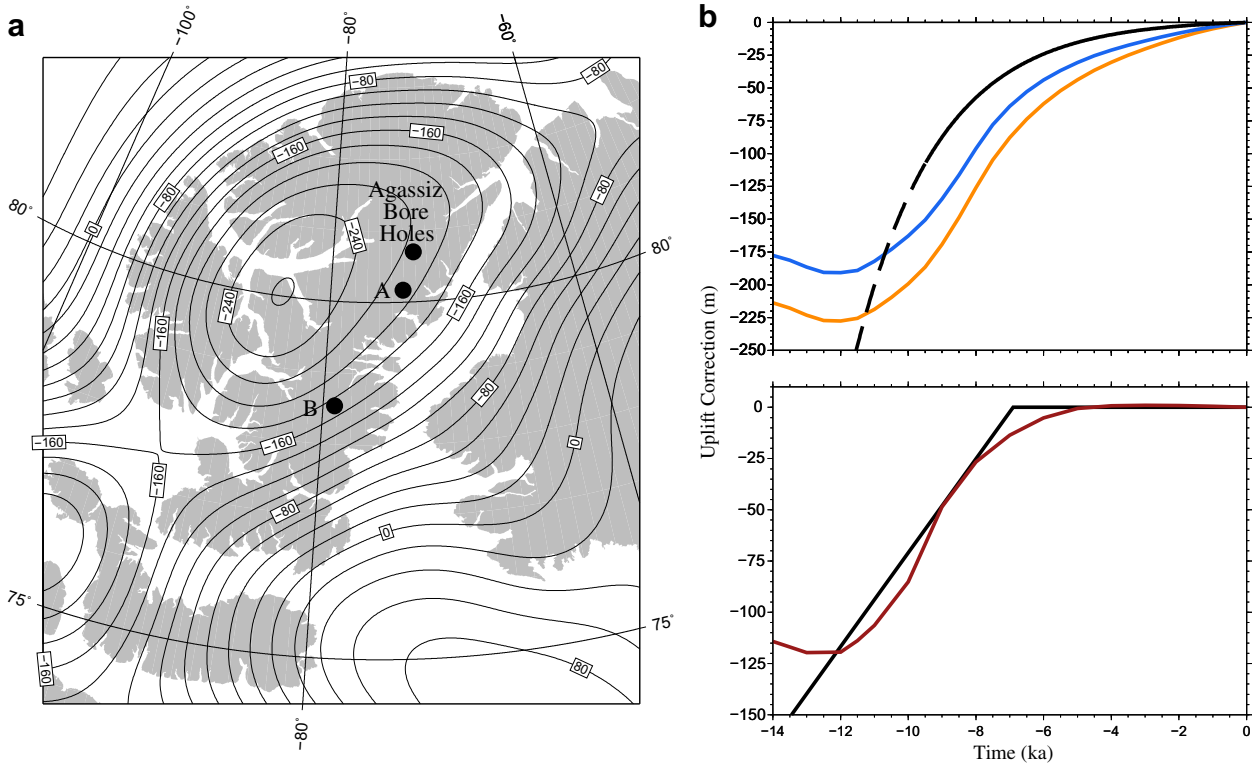

Fig. 4. (a) The spatial variability in GIA-induced uplift of Ellesmere Island at 10 ka BP using the optimal Earth model. The plot shows the location of the Agassiz ice cap core locations (A87 and A84, both at the dome) along with the two sites at which uplift was predicted (A, B). (b) Top frame shows predicted uplift curves generated using the optimal Earth model at the two locations (A, B; orange, blue, respectively) shown in (a). Also shown is the uplift curve adopted by Vinther et al. (2009) (black). Bottom frame shows the Renland original uplift correction applied in Vinther et al. (2009) (black) along with the uplift curve generated using the optimal model (red) from Simpson et al. (2009) (see text for details). (For interpretation of the references to colour in this figure legend, the reader is referred to the web version of this article.)

was measured using an altimeter and have an estimated uncertainty of ±1 m for markers below 20 m in elevation and ±5% for indicators above 20 m (Blake, 1999; Dyke and Peltier, 2000). The curves were computed using the ICE-5G ice model and an Earth model which produced the best fit for Ellesmere Island RSL data; lithosphere thickness of 71 km, upper mantle viscosity of 0.3×10^{21} Pa s, and lower mantle viscosity of 10^{21} Pa s. We also considered observations from north–west Greenland and Devon Island and the optimal Earth models obtained for these regions are compatible (within the 95% confidence range) with those inferred from Ellesmere Island. This suggests that there are no large gradients in Earth structure that influences the GIA signal in the region and so the use of a 1D Earth model is appropriate. Using the Huy2 model within ICE-5G, the optimal Earth model parameters obtained using the Greenland data were also compatible with those inferred using the original ICE-5G ice model. This indicates that our viscosity inference for Agassiz is not strongly affected by the adopted Greenland ice model component (i.e. Huy2 vs GrB).

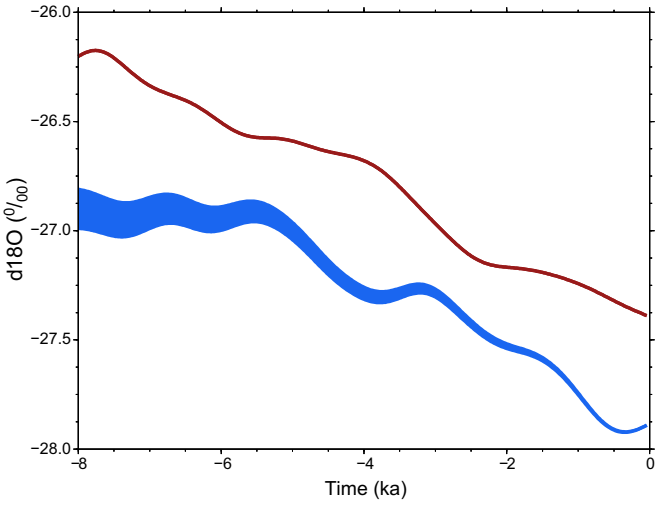

Fig. 5. The Agassiz (site A and B acceptable range; blue) and Renland (red) gaussian filtered $\delta^{18}O$ records corrected for land uplift. For Agassiz, the curves predicted at the two chosen locations were applied: site A (top) and site B (bottom). A $\delta^{18}O$ profile is interpolated/extrapolated across Greenland using the uplift-corrected and height synchronized Agassiz and Renland curves. (For interpretation of the references to colour in this figure legend, the reader is referred to the web version of this article.)

The data-model fits shown in Fig. 3 (a, b) are generally of high quality, with the predicted curve bisecting the limiting dates as required. There are two sites (9 & 12) where the data-model residual is substantial (more than ~10 m) as the modelled curve sits too low. This could relate to inaccuracies in the adopted ice loading model or limitations in the Earth model (e.g. the assumption of 1-D structure). Regardless of the source of the residual at these two sites, a key point is that the locations chosen to compute the uplift corrections for the Agassiz $\delta^{18}O$ record are in the vicinity of sites 3 and 7, where the model fits are compatible with the data to within uncertainty (compare Figs. 2 and 4a).

As outlined above, choosing a location to apply the uplift correction for the Agassiz cores is difficult, since the moisture pathways are not well constrained in space and time. The limitations of high resolution atmospheric modelling over timescales of thousands of years do not permit the use of this approach to identify the most common pathways by which the air mass was carried from Baffin Bay to the Agassiz ice cap during the Holocene. As a result, we focus here on placing a bound on the range of uplift curves that can

be applied to the Agassiz ice core data. This range can then be used to define an uncertainty on the GIA-induced land uplift signal in the Agassiz ice cap $\delta^{18}O$ record. As shown in Fig. 4a, there is considerable spatial variability in the predicted amplitude of land uplift along the east coast of Ellesmere Island. Two sites (A & B, Fig. 4a) were chosen to evaluate the uplift correction for Agassiz as they correspond to topographic highs that bound the most likely pathways over which moisture could have been transported before precipitating over the Agassiz ice cap, while taking into account changes in sea-ice cover through time (England et al., 2006, 2008). Uplift at site B was likely the dominant control on Agassiz $\delta^{18}O$ during the early to mid-Holocene after the Innuitian ice sheet thinned enough to expose the underlying high terrain and when greater sea ice cover would have resulted in more southerly moisture pathways. The predicted uplift curves for sites A and B are shown in Fig. 4b along with the curve used by Vinther et al. (2009). We note that there are differences of up to ~100 m between the revised curves and that estimated in the original analysis.

Using RSL data from east Greenland, Simpson et al. (2009) found an optimal Earth model (to partner their Huy2 ice model) with a lithospheric thickness of 120 km and upper and lower mantle viscosities of 0.3×10^{21} Pa s and 5.0×10^{22} Pa s, respectively. This Earth model provided the best fit to the data at their sites 11–17 (see their Figs. 1 and 16 of Simpson et al., 2009). We adopted the Simpson et al. ice model (ICE-5G revised to contain Huy2) and this Earth model to generate a land uplift curve at the location of the Renland ice core (Fig. 4b). This new uplift curve is similar to that adopted in the original Vinther et al. analysis.

The results in Fig. 4b indicate that the total amplitude of the uplift-correction for the Agassiz $\delta^{18}O$ record can range from ~ − 220 m (Site A) to ~ − 150 m (Site B). In order to determine the influence of this range on the estimated ice elevation curves at the GrIS ice core sites, we follow the general procedure adopted by Vinther et al. but use the two end member Agassiz uplift curves to incorporate the uncertainty introduced by this issue. As discussed above, neither $\delta^{18}O$ records from Agassiz nor Renland are believed to have experienced significant changes in $\delta^{18}O$ as a result of changes in ice thickness over the Holocene. Therefore, once their respective $\delta^{18}O$ records are corrected for changes in land elevation (see Fig.5) and other processes (see Section 1.2), the resulting time series represents a proxy for surface air temperature changes at each locality (Vinther et al., 2009).

During the early Holocene, the Innuitian ice sheet was quite extensive in southern Ellesmere Island. As a consequence, it likely affected the predominant moisture pathways and, therefore, the correction to be applied to the Agassiz $\delta^{18}O$ record. Quantifying the effect of this ice is not straightforward, however. It might have shifted the location where the elevation correction is to be applied and also increased the elevation to which the air moisture was elevated to. Based on field evidence (England et al., 2006, 2008), the Innuitian ice sheet reduced significantly in vertical extent along the south east coast of Ellesmere Island until approximately 8 ka BP. In the ICE-5G reconstruction, ice thickness in southern Ellesmere reaches present-day values around 8 ka BP. Therefore, the influence of the ice was likely only significant during the early Holocene (and certainly prior to 8 ka BP). We raise this issue only to make the point that the elevation corrections for Agassiz ice (Fig. 4b) might require revision for the period prior to 8 ka BP. Quantifying this revision requires the application of high resolution atmospheric modelling as well as accurate reconstructions of ice extent in this region. This work is beyond the scope of this study. Qualitatively the addition of the Innuitian ice to existing topography will, however, result in an increased topographic barrier or/and a longer moisture pathway. Both effects are likely to cause further depletion of $\delta^{18}O$ in precipitation at the Agassiz drill site, thus dominating the effect over the uplift curves presented in Fig. 4b during the early Holocene. The resulting impact of the Innuitian ice sheet on the thinning curves will likely be a greater thinning rate at GRIP, NGRIP, and Camp Century and a decreased rate at DYE-3, which would act, in general, to increase the discrepancy between the thinning curves and model reconstructions noted in the original analysis. However, incorporating the influence of this effect into the analysis will result in a large amplification of the uncertainty in the early part (12 ka–8 ka) of the estimated thinning curves.

3.2. AR temperature records

A temperature reconstruction is conducted on both the AR records. Since the $\delta^{18}O$ records from these ice caps haven't been drastically influenced by changes in ice thickness (especially during the late Holocene), once the vertical land motion correction is applied, a relatively untainted mid to late Holocene temperature reconstruction at high latitudes is obtained (Fig. 6). These temperature records relate the temperature history for an absolute height (ice cap surface) relative to sea-level through time. The Agassiz temperature record could be used to assess the accuracy of the uplift correction applied if interpreted with the Agassiz melt record (Fisher et al., 1995), since both records should agree on the timing of the HTM. The AR temperature record has further applications in reconstructions of the Greenland ice sheet through glaciological modelling studies. Most numerical ice sheet models of Greenland use the GRIP temperature record to force the ice sheet by extrapolating the record over Greenland (e.g. Huybrechts, 2002), however, there are few temperature reconstructions from the ice margin that can be used to validate the accuracy of the extrapolation scheme.

3.3. Revised Holocene thinning curves

As discussed above, a spatially variable (linear) $\delta^{18}O$ profile is applied since the AR uplift corrected records differ by a significant amount (Fig. 5), especially after height synchronization. Following the method outlined in Section 2.2, site specific $\delta^{18}O$ profiles are calculated for GRIP, NGRIP, DYE-3 and Camp Century based on the

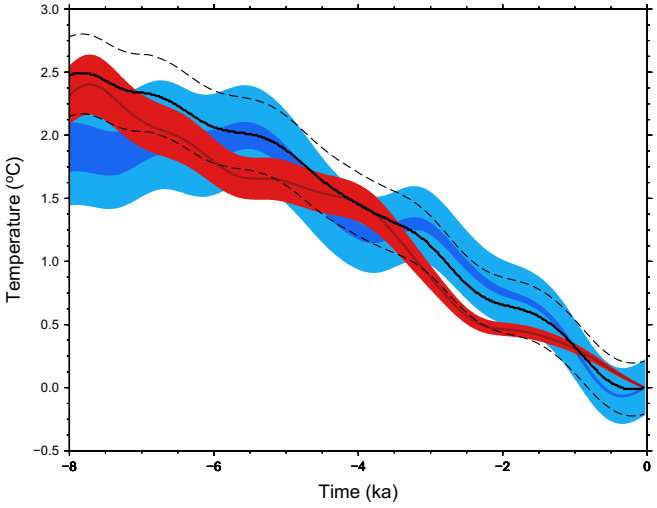

Fig. 6. Temperature reconstruction at the Agassiz (blue) and Renland (red) ice caps are obtained by correcting the uplift corrected $\delta^{18}O$ from AR (Fig. 5), for changes in the ocean's $\delta^{18}O$ content and applying the $^{\circ}C/\delta^{18}O$ slope of 2.1 ± 0.2 $^{\circ}C/\delta^{18}O$. The original temperature reconstruction for the whole Greenland region from the Vinther et al. analysis is shown in black. (For interpretation of the references to colour in this figure legend, the reader is referred to the web version of this article.)

uplift-corrected AR records. In Fig. 7, the revised ice surface elevation curves (coloured) are shown with those from the original Vinther et al. analysis (black). In general, the new uplift corrections result in a decreased overall amplitude to the thinning curves with similar characteristics and introduce uncertainty – one that increases with time (max of ±26 m) – due to the lack of a specific location at which to apply the Agassiz uplift correction. The revised thinning curves generally remain within the 1-sigma uncertainty of the original analysis, except for periods during the early Holocene. The differences between the old and new thinning curves reflect the relative importance of the AR records on each site, the records applied to correct them and their interpretation. The $\delta^{18}O$ profile has the greatest impact on the DYE-3 thinning curves since the new extrapolated site specific $\delta^{18}O$ record emphasizes and amplifies differences in the AR corrected $\delta^{18}O$ record (see Fig. 1a).

As stated above, rather than average the AR records, we calculate a (linear) spatial gradient in $\delta^{18}O$ between the AR $\delta^{18}O$ records. To determine the uncertainty associated with this procedure, we compare the gradient estimated from the uplift-corrected and elevation synchronised (using −0.6‰ per 100 m) AR $\delta^{18}O$ records to that estimated from Greenland ice cores, −0.54‰ per degree North (Johnsen and White, 1989). Since the thinning curves are obtained with the use of these empirical latitudinal and elevational relationships, it is appropriate to quantify the accuracy of our results based on their consistency with these relationships.

An additional error is introduced by the two Agassiz ice cores, A87 and A84, producing a further uncertainty of ±16 m at all sites. The error associated with DYE-3 and Camp Century is larger due to contributions from less precise $\delta^{18}O$ measurements in core layers at these locations producing an additional error of ±25 m. Combining these error sources quadratically leads to the total maximum 1-σ uncertainty (lighter coloured shading in Fig. 7) respectively being ± 68, 68, 72, and 72 m for GRIP, NGRIP, DYE-3, and Camp Century. These uncertainty ranges are somewhat larger than those for the original curves and result in a poorer signal to noise ratio, particularly for the period 8 ka BP to present.

3.4. Comparison of thinning curves to output from numerical ice models

The Holocene thinning curves are a unique observational constraint that can be compared to output from numerical ice sheet models. To date, this type of information has only been available through identifying and dating geomorphological features such as trim lines that are generally found in proximity to the ice margin. Fig. 8 shows the new thinning curve at the present summit of the GrIS (GRIP) as well as output from 3D numerical ice sheet models (Huybrechts, 2002; Tarasov and Peltier, 2002; Greve, 2005; Lhomme et al., 2005; Simpson et al., 2009). The model fits are improved relative to the original thinning curve and three models capture the thinning for the period 8 ka BP to present. Results from the Lhomme et al. (2005), Huybrechts (2002) and Simpson et al. (2009) models are closest to the estimated thinning curve. We note that the Huy2 model is an extended version of the Huybrechts (2002) model, calibrated to fit both a regional RSL data set and field constraints on ice extent. However, there still exists discrepancy during the early Holocene, although this section of the curve could change significantly. All models result in a considerable elevation increase during the early Holocene, except for the Huy2 reconstruction which shows a relatively stable ice surface throughout the Holocene.

The model misfits illustrated in Fig. 8 for some models and not others bring into question the accuracy of the current generation of deglacial GrIS reconstructions obtained from numerical ice models. It is important to determine the sources of the discrepancy, which likely include both the ice models (in terms of the processes simulated, model parameterisation, and numerical accuracy) and data employed to constrain model input (e.g. climate) and output

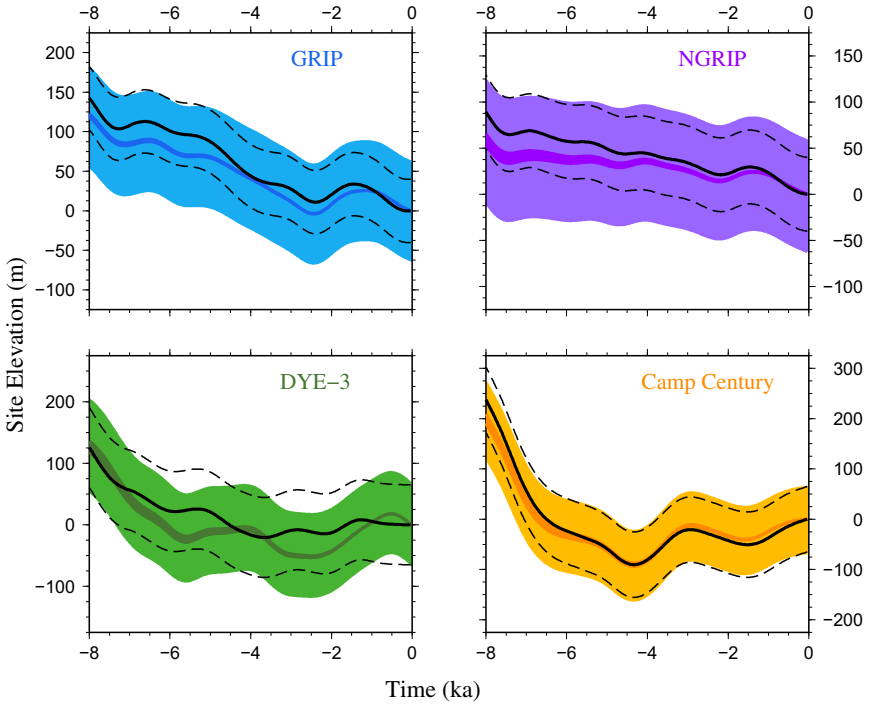

Fig. 7. Ice elevation curves at four Greenland ice core locations (Fig. 1a). The original results of Vinther et al. (2009) are displayed (solid black line) along with the 1-σ uncertainty (dashed black line). The newly derived curves define a range of values associated with the two different uplift curves for Agassiz (site A & B in Fig. 2a); this range is indicated (darker coloured band) along with the estimated 1-σ uncertainty (lighter coloured band).

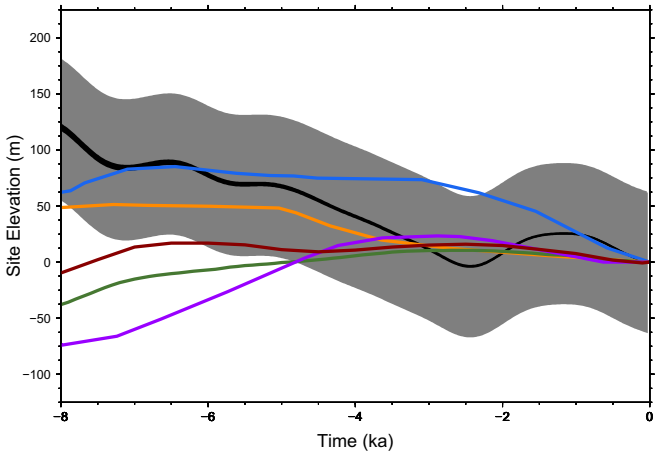

Fig. 8. (a) Comparison of the newly derived thinning curve (black; uncertainty bound indicated by grey band) at the GRIP drill site with output from three-dimensional thermomechanical models of the GrIS (orange, Huybrechts (2002); blue, Lhomme et al. (2005); green, Greve (2005); purple, Tarasov and Peltier (2002); red, Simpson et al. (2009)). (For interpretation of the references to colour in this figure legend, the reader is referred to the web version of this article.)

(e.g. ice extent). This task requires multiple lines of investigation using numerical ice sheet models with increasing degrees of sophistication to incorporate effects such as grounding line migration, longitudinal stresses, ice-ocean heat exchange (e.g. Pollard and Deconto, 2009). Given that a key aspect of the current study is modelling vertical land motion, we briefly consider limitations in this aspect of the calculation in computing the contribution of vertical land motion to the modelled ice surface elevation changes in Fig. 8. The treatment of isostasy in an ice model will affect both the output of ice extent through time (e.g. Le Meur and Huybrechts, 1996; Van de Berg et al., 2008) as well as computations of vertical land motion for a given ice load distribution history. It is the latter that we consider here.

In Fig. 9 we show ice surface elevation curves at all four core sites for the Huy2 ice model. Two model curves are shown that are based on the same ice model reconstruction but adopt different treatments of isostasy and loading functions in the land height change component of the surface elevation changes. The dashed black line is based on a treatment of isostasy that is commonly employed in numerical ice sheet models (essentially, elastic plate flexure that incorporates viscous mantle flow by introducing a single response or relaxation time; see, for example, Le Meur and Huybrechts, 1996). In this case, the loading model comprises the Greenland ice sheet reconstruction and a eustatic ocean load. The solid black line is based on more complex Earth and loading models commonly applied in GIA analyses. The Earth model is a spherically symmetric, self-gravitating, Maxwell body and includes both elastic and non-elastic response components, with the latter defined by a spectrum of decay times and amplitudes that vary for different wavelengths of deformation (e.g. Peltier, 1974; Le Meur and Huybrechts, 1996). The loading model includes a gravitationally-self consistent ocean load (Farrell and Clark, 1976; Mitrovica and Milne, 2003) and a global reconstruction of ice loading changes (ICE-5G minus GrB) in addition to the Greenland ice component (Huy2). Inspection of Fig. 9 shows that the more realistic model results in an increased surface lowering at all core sites. This difference is dominated by the loading influence of non-Greenland ice (largely North American ice) leading to land subsidence of 30–40 m throughout the Holocene. While the application of this more realistic loading and Earth deformation model certainly acts to improve the fit at each site, there remains significant discrepancy at the sites closest to the margin (Camp Century and DYE-3). Those at Camp Century could be related to enhanced pre-Holocene thickening at this site due to the confluence of the Greenland and Innuitian ice sheets, while those at Dye-3 could be related to the high amplitude and short wavelength terrain in this area which are not well captured in the Huy2 ice model.

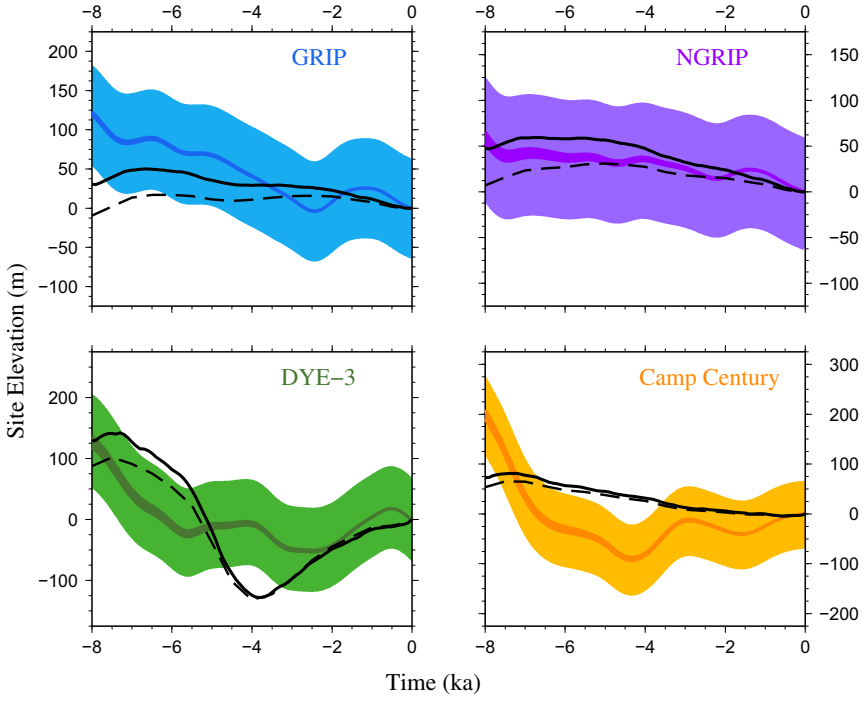

Fig. 9. Comparison of the Huy2 Greenland ice model (solid black) used in this study with the new Holocene thinning curves. The dashed black line is the predicted ice surface elevation change when the land height signal is computed using the isostasy treatment in the ice model. The solid black line is the predicted elevation change when the land height signal is computed using a more sophisticated treatment of isostasy (in terms of the loading and the Earth deformation). See text for details.

With respect to the ice-core analysis and the resulting elevation histories, interpreting the $\delta^{18}O$ variations as elevation changes at GRIP, NGRIP, DYE-3 and Camp Century is an aspect of the study that should be refined as more studies investigate $\delta^{18}O$ differences amongst northern hemisphere ice cores. The relatively simplistic empirical relationships employed in this study (linear dependence of ‰ $\delta^{18}O$ with latitude and altitude does not capture the complexities of $\delta^{18}O$ variability across the region and so further studies to quantify these relationships would improve the accuracy and precision of the inferred thinning curves. Also, if total gas content of the NGRIP was measured, we could validate the thinning history at the NGRIP site (Vinther et al., 2009). The above analysis could be improved through obtaining better constraints on dominant moisture sources and pathways for precipitation on the Agassiz ice cap. This is particularly important for the early portion of the curve (12–8 ka BP) when the largest changes likely occurred and the influence of Innuitian ice could have been significant.

4. Conclusion

We revisited the analysis of Vinther et al. (2009) to determine if the use of more accurate land uplift corrections for the $\delta^{18}O$ records from the AR ice caps would result in a significant difference to the inferred ice surface thinning histories at Greenland ice core sites. The primary motivation of this exercise was to determine if changing this aspect of the original analysis could account for the large discrepancy between the original thinning curves and output from numerical ice models. We applied uplift histories that were computed using a GIA model calibrated to sea-level observations from Arctic Canada and Greenland. Removing the land height signal from the Agassiz $\delta^{18}O$ record is complicated by the fact that the specific locality to apply this correction is not accurately known, this is due to uncertainty in the moisture pathways and the possible influence of Innuitian ice prior to ~8 ka BP (the latter issue is not quantified in this analysis). The new thinning curves for the period 8 ka BP to present are, in general, shifted down relative to the original curves at GRIP, NGRIP, DYE-3 and Camp Century. In addition, compared to the original analysis, the 1-σ uncertainty is considerably larger at GRIP and NGRIP. These changes reduce the data-model discrepancy reported by Vinther et al. (2009) at the Greenland core sites. A more accurate treatment of isostasy and surface loading also acts to improve the data-model fits such that the residuals at all sites for the period 8 ka BP to present are significantly reduced compared to the original analysis. Prior to 8 ka BP, the possible influence of Innuitian ice on the inferred elevation histories prevents a meaningful comparison. Incorporating this component into the analysis is a prime target for future investigation.

Acknowledgements

This work was funded by the Natural Sciences and Engineering Research Council of Canada. We thank Lev Tarasov for useful discussions related to the work presented in this paper. The work presented here benefitted significantly from discussions during two PALSEA workshops (PALSEA is a working group funded through PAGES/INQUA/WUN).

References

Blake Jr., W., 1999. Glaciated landscapes along Smith Sound, Ellesmere Island, Canada and Greenland. Annals of Glaciology 28, 40–46.

Buchardt, S.L., Dahl-Jensen, D., 2007. Estimating the basal melt rate at NorthGRIP using a Monte Carlo technique. International Symposium on Earth and Planetary Ice-Volcano Interactions, Jun 19–23, 2006 Univ Iceland, Inst Earth Sci, Reykjavik, Iceland. Annals of Glaciology 45, 137–142.

Dahl-Jensen, D., Johnsen, S.J., 1986. Palaeotemperatures still exist in the Greenland ice-sheet. Nature 320, 250–252.

Dahl-Jensen, D., Mosegaard, K.E., Gundestrup, N.S., Clow, G.D., Johnsen, S.J., Hansen, A.W., Balling, N., 1998. Past temperatures directly from the Greenland ice sheet. Science 282, 268–271.

Dahl-Jensen, D., Gundestrup, N.S., Gogineni, S., Miller, H., 2003. Basal melt at NorthGRIP modeled from borehole, ice-core and radio-echo sounder observations. Annals of Glaciology 37, 207–212.

Dansgaard, W., 1961. The isotopic composition of natural waters. Meddelelser Om Grψnland 165, 2.

Dyke, A.S., Peltier, W.R., 2000. Forms, response times and variability of relative sea-level curves, glaciated North America. Geomorphology 32, 315–333.

Dziewonski, A.M., Anderson, D.L., 1981. Preliminary reference Earth model. Physics of the Earth and Planetary Interiors 25, 297.

England, J., Atkinson, N., Bednarski, J., Dyke, A.S., Hodgson, D.A., Ó Cofaigh, C., 2006. The Innuitian Ice Sheet: configuration, dynamics and chronology. Quaternary Science Review 25, 689–703.

England, J.H., Lakeman, T.R., Lemmen, D.S., Bednarski, J.M., Steward, T.G., Evans, D.J.A., 2008. A millennial-scale record of Arctic Ocean sea ice variability and the demise of the Ellesmere Island ice shelves. Geophysical Research Letters 35, L19502.

Farrell, W.E., Clark, J.A., 1976. On postglacial sea level. Geophysical Journal of the Royal Astronomical Society 46, 647–667.

Fisher, D.A., 1990. A zonally-averaged stable-isotope model coupled to a regional variable-elevation stable-isotope model. Annals of Glaciology 14, 65–71.

Fisher, D.A., 1992. Stable isotope simulations using a regional stable isotope model coupled to a zonally averaged global model. Cold Regions Science and Technology 21, 61–77.

Fisher, D.A., Koerner, R.M., Reeh, N., 1995. Holocene climatic records from Agassiz Ice Cap, Ellesmere Island, NWT, Canada. Sage 5, 19–24.

Funder, S., 1978. Holocene stratigraphy and vegetation history in the Scoresby Sund area, east Greenland, Grønl. Geologiske Undersoekels Bulletin 129.

Greve, R., 2005. Relation of measured basal temperatures and the spatial distribution of the geothermal heat flux for the Greenland ice sheet. Annals of Glaciology 42, 424–432.

Gundestrup, N.S., Dahl-Jensen, D., Johnsen, S.J., Rossi, A., 1993. Bore-hole survey at dome GRIP 1991. Cold Regions Science and Technology 21, 399–402.

Huybrechts, P., 2002. Sea-level change at the LGM from ice-dynamics reconstructions of the Greenland and Antarctic ice sheets during the glacial cycles. Quaternary Science Review 21, 203–231.

Johnsen, 1977. Stable isotope profiles compared with temperature profiles in firn with historical temperature records. In: Proc. Symp. On Isotopes and Impurities in Snow and Ice. I.U.G.G. XVI, General Assembly, Grenoble, pp. 388–392. 1975.

Johnsen, S.J., White, J.W.C., 1989. The origin of Arctic precipitation under present and glacial conditions. Tellus 41B, 452–468.

Johnsen, S.J., Clausen, H.B., Dansgaard, W., Gundestrup, N.S., Hansson, M., Jonsson, P., Steffensen, J.P., Sveinbjφrnsdottir, A.E., 1992. A deep ice core from east Greenland. Meddelelser Om Grψnland 29, 3–29.

Koerner, R.M., 1979. Accumulation, ablation, and oxygen isotope variations on the Queen Elizabeth Islands ice caps, Canada. Journal of Glaciology 22 (86), 25–41.

Koerner, R.M., Fisher, D.A., 1990. A record of Holocene summer climate from a Canadian high Arctic ice core. Nature 343 (6259), 630–631.

Le Meur, E., Huybrechts, P., 1996. A Comparison of different ways of dealing with isostasy: examples from modeling the Antarctic ice sheet during the last glacial cycle. Annals of Glaciology 23, 309–317.

Lhomme, N., Clarke, G.K.C., Marshall, S.J., 2005. Tracer transport in the Greenland ice sheet: constraints on ice cores and glacial history. Quaternary Science Review 24, 173–194.

Milne, G.A., Mitrovica, J.X., 1998. Postglacial sea-level change on a rotating Earth. Geophysical Journal International 133, 1–19.

Mitrovica, J.X., Milne, G.A., 2003. On post-glacial sea level. Geophysical Journal International 154, 253–267.

Peltier, W.R., 1974. The impulse response of a Maxwell Earth. Reviews of Geophysics and Space Physics 12, 649–669.

Peltier, W.R., 2004. Global glacial isostasy and the surface of the ice-age Earth: the ICE-5G (VM2) model and GRACE. Annual Review of Earth and Planetary Sciences 32, 111–149.

Pollard, D., Deconto, R., 2009. Modelling West Antarctic ice sheet growth and collapse through the past five million years. Nature 458 (7236), 329–332.

Reeh, N., Johnsen, S.J., Dahl-Jensen, D., 1985. Dating the DYE-3 deep ice core by flow model calculations. In: Geophysical Monograph, vol. 33. American Geophysical Union, pp. 57–65.

Simpson, M.J.R., Milne, G.A., Huybrechts, P., Long, A.J., 2009. Calibrating a glaciological model of the Greenland ice sheet from the last glacial maximum to present-day using field observations of relative sea level and ice extent. Quaternary Science Reviews 28, 1630–1656.

Tarasov, L., Peltier, W.R., 2002. Greenland glacial history and local geodynamic consequences. Geophysical Journal International 150 (1), 198–229.

Van de Berg, J., Van de Wal, R.S.W., Milne, G.A., Oerlemans, J., 2008. Effect of isostasy on dynamical ice sheet modeling: a case study for Eurasia. J. Geophys. Res 113, B05412.

Vialov, 1958. Regularities of glacial ice shields movement and the theory of glaciers. International Association of Scientific Hydrology Publication 47, 266–275.

Vinther, B.M., Clausen, H.B., Johnsen, S.J., Rasmussen, S.O., Andersen, K.K., Buchardt, S.L., Dahl-Jensen, D., Seierstad, I.K., Siggaard-Andersen, M.L., Steffensen, J.P., Svensson, A., Olsen, J., Heinemeier, J., 2006. A synchronized dating of three Greenland ice cores throughout the Holocene. Journal of Geophysical Research 111, D13102.

Vinther, B.M., Clausen, H.B., Fisher, D.A., Koerner, R.M., Johnsen, S.J., Andersen, K.K., Dahl-Jensen, D., Rasmussen, S.O., Steffensen, J.P., Svensson, A.M., 2008. Synchronizing ice cores from the Renland and Agassiz ice caps to the Greenland Ice Core Chronology. Journal of Geophysical Research 113, D08115.

Vinther, B.M., Buchardt, S.L., Clausen, H.B., Dahl-Jensen, D., Johnsen, S., Fisher, D.A., Koerner, R.M., Raynaud, D., Lipenkov, V., Andersen, K.K., Blunier, T., Rasmussen, S.O., Steffensen, J.P., Svensson, A.M., 2009. Holocene thinning of the Greenland ice sheet. Nature 461, 385–388.

Waelbroeck, C., Labeyrie, L., Michel, E., Duplessy, J.C., McManus, J.F., Lambeck, K., Balbon, E., Labracherie, M., 2002. Sea-level and deep water temperature changes derived from benthic foraminifera isotopic records. Quaternary Science Reviews 21, 295–305.